PNAS
www.pnas.org

Supplementary Information for

NETosis proceeds by cytoskeleton and endomembrane disassembly and PAD4-mediated chromatin de-condensation and nuclear envelope rupture

Hawa Racine Thiam[1*], Siu Ling Wong[2*#], Rong Qiu[4], Mark Kittisopikul[4,5], Amir Vahabikashi[4], Anne E. Goldman[4], Robert D. Goldman[4], Denisa D. Wagner[2,3*], Clare M. Waterman[1*]

[1]Cell Biology and Physiology Center, NHLBI, NIH; [2] Program in Cellular and Molecular Medicine, Boston Children's Hospital Boston, MA 02115; Department of Pediatrics, Harvard Medical School, Boston, MA 02115; [3] Division of Hematology/Oncology, Boston Children's Hospital Boston, MA 02115. [4]Department of Cell and Molecular Biology, Northwestern University Feinberg School of Medicine, Chicago IL 60611; [5]Department of Biophysics, UT Southwestern Medical Center, Dallas, TX 75390

Clare M. Waterman
Email: watermancm@nhlbi.nih.gov

This PDF file includes:

Materials and Methods
Figures S1 to S6
Legends for Movies S1 to S22
SI References

www.pnas.org/cgi/doi/10.1073/pnas.1909546117

MATERIALS AND METHODS

Cells:

HL-60 cell differentiation and transfection: HL-60 cells were purchased form ATCC (ATCC® CCL-240™), cultured at 37°C and 5% CO_2 in RPMI 1640 with L-glutamine (ThermoFisher, 11875093) with 25 mM HEPES (ThermoFisher, 15630080), 1% (P/S; ThermoFisher, 10378016) and 15% heat-inactivated Fetal bovine Serum (FBS; Atlanta Biologicals, S11150) and split every 2 days at 3.10^5 cells/mL. Cells were differentiated with culture media supplemented with 1.3% DMSO (Sigma, D2650) as previously described (1). Differentiated cells (dHL-60) were used 6 or 7 days after onset of differentiation. Transient expression of cDNA was performed by electroporating 2 µg of DNA in $2x10^6$ cells using the Amaxa nucleofector kit V (Lonza, VCA-1003) and the program Y-001 on an Amaxa Nucleofector II (Lonza). Differentiated cells were imaged 6 hours after transfection. HL-60 cells stably expressing F-tractin-mApple were generated by transfecting $2x10^6$ non-differentiated HL-60 cells with 2 µg of DNA. Transfected cells were selected with 1 mg/mL of G418 for 2 weeks before being sorted by flow cytometry for mApple positive cells. All live cell imaging was performed with imaging media: RPMI 1640 lacking Phenol red (Fisher scientific, 11835030) with 25 mM HEPES and 1% P/S.

Isolation of mouse neutrophils: Neutrophils were isolated from the fresh blood of WT and PAD4 KO mice as previously described (2). Briefly, the mice were bled for 1 mL via the retro-orbital plexus into 2 mL anti-coagulant (15 mM EDTA and 1% BSA in sterile PBS) after being deeply anesthetized with isoflurane. The blood was centrifuged at 2,400 rpm for 12 min at room temperature, the supernatant was removed, and cells were resuspended in anti-coagulant before loading on top of a percoll gradient column of 52%/69%/78%, with 78% being the lowest layer in the 15 mL centrifuge tube. The column was then centrifuged at 1,500 x g for 32 min at room temperature with acceleration set at 3 and deceleration set at 0. Cells at the 69%/78% interface were collected and pelleted with addition of PBS at 500 x g for 12 min at room temperature. Cells were then subjected to a brief water lysis, and the majority of the red blood cells were removed after the osmotic challenge. The neutrophils were then resuspended in imaging media, either stained with SiR-DNA, SiR-Actin, SiR-Tubulin or ER-Tracker Red dye according to manufacturers' directions for immediate live imaging, or plated onto coverslips and stimulated for NETosis, and thereafter fixed for immunostaining.

Isolation of human blood neutrophils: Human blood samples were obtained from healthy donors on NIH IRB-approved protocol 99-CC-0168. Research blood donors provided written informed consent and blood samples were de-identified prior to distribution. Neutrophils isolation was performed as described in (3). Briefly, 6 mL of blood was layered on 6 mL of Histopaque-1119 (Sigma-Aldrich, 11191) then spun down at 1100 g for 22 min at 24°C; acceleration 2, deceleration 1. After removal of the plasma and leukocyte layer, the granulocytes/erythrocytes layer was washed with HBSS (Gibco™ HBSS without Calcium, Magnesium or Phenol Red; ThermoFisher, 14175095) by centrifugation (400 g; 10 min; 23°C; acceleration 9; deceleration 9). The resulting pellet was resuspended in 2 mL of HBSS then layered on a percoll (Percoll Plus, GE Healthcare, 17-5445-02) gradient column of, from bottom to top, 85%/80%/75%/70%/65% percoll in PBS (DPBS, no calcium, no magnesium; ThermoFisher, 14190144) before being centrifuged at 1100 g for 23 min at 23°C; acceleration 2, deceleration 1. The neutrophil layer (from the middle of the 70% to the middle of the 80% percoll layer) was washed with HBSS by centrifugation (400 g; 11 min; 23°C; acceleration 9; deceleration 9). The pellet was resuspended in 1 mL HBSS before being counted. Cells were resuspended at 10^3 cells/µL in imaging media and $3x10^5$ cells were either stained with SiR-DNA, SiR-Actin, SiR-Tubulin or ER-Tracker Red dye according to manufacturers' directions for live cell imaging or plated on coverslips for immunostaining.

Candida albicans culture: dTomato-expressing *C. albicans* (strain CAF2-1-dTomato) were a kind gift of Mihail Lionakis (NIAID, NIH, Bethesda). Frozen cell stock were plated on YPD/agar, incubated overnight at 37C, and a single colony was inoculated in YPD media supplemented with 1% Penicillin and Streptomycin (P/S; ThermoFisher, 10378016). Liquid culture was grown overnight at 30°C in a shaker incubator, diluted 1:10, grown for 3 more hrs to eliminate dead cells before being opsonized with 10% human serum, washed and used for microscopy at MOI of 2.

cDNA Expression Vectors:

cDNAs encoding CaaX-mApple, H1-mEmerald, ER-5-mEmerald, Lamin B1-mApple, Lamin A-mEmerald, F-tractin-mApple, G-actin-mEmerald, Tubulin-mEmerald, Vimentin-mEmerald, H2B-mEmerald and mEmeral-C1 were the kind gift of the late Mike Davidson (Florida State University, Tallahassee, FL); eGFP-Ensconsin (3X-GFP-EMTB) was a kind gift from Chloe Bulinski (Columbia University, New York, NY); pSpCas9-2A-GFP vector (Addgene, 48138 (4)) was a kind gift from James Anderson's Lab (NHLBI/NIH, Bethesda, MD).
To generate the PAD4-mEmerald vector, human PAD4 cDNA was purchased from Sino Biological Inc. (pCMV3-N-His-PADi4, HG11072-NH). The PADi4 mRNA was PCR amplified with primers containing the KpnI and BamHI restriction sites (Fw1: 5'-CCG GGT ACC GCC CAG GGG ACA TTG ATC CG-3'; Rev1: 5'-GGT GGA ACA TGG TGC CCT AAG GAT CCC CG-3'). The so obtained PAD4 insert and the mEmerald-C1 vector were cut with restriction enzymes (KpnI, BamHI, New England Biolabs) then ligated together with T4 DNA ligase (ThermoFisher, EL001) after dephosphorylation with Calf Intestinal Alkaline Phosphatase (CIAP; ThermoFisher, 18009019) of the linearized plasmid and gel purification (QIAquick Gel Extraction Kit; Quiagen, 28706) of both insert and vector. DH5α competent cells (ThermoFisher, 18258012) were transformed with 5 µL of the ligation product. Kanamycin (ThermoFisher, 15160054) resistant colonies were further amplified and minipreps (Quiagen; 27106) were performed. The obtained mEmerald-PAD4 plasmids were cut with the restriction enzymes KpnI and BamHI to verify the presence of a 2 kbp and 4.7 kbp products testing the overall integrity of the plasmid. The insert was further verified by full sequencing.
The enzymatically dead (mEmerald-PAD4-C645A) and the NLS dead (mEmerald-PAD4-K59A/K60A/K61A) mutants were generated based on (5) and (6) respectively by *in vitro* site-directed mutagenesis using the QuikChange II XL Site-Directed Mutagenesis Kit (Agilent, 200521) as directed by the manufacturer. Briefly, appropriate mutations were introduced to the mEmerald-PAD4 vector by PCR amplification using following primers: K59-60-61A-Fw: 5'-CCA TGT GGA GGA ACC TGT GGA TGC CGC CGC GGC TGG AGG GCC GTG GGC AAT A-3'; K59-60-61-Rev: 5'-TAT TGC CCA CGG CCC TCC AGC CGC GGC GGC ATC CAC AGG TTC CTC CAC ATG G-3'; C645A-Fw: 5'-CAC GTT GGT GCC GGC GTG CAC CTC CCC A-3'; C645A-Rev: 5'-TGG GGA GGT GCA CGC CGG CAC CAA CGT G-3'. The PCR amplification products were incubated with DpnI restriction enzyme to digest the parental methylated and hemimethylated DNA (mEmerald-PAD4) before being used to transform XL10-Gold Ultracompetent Cells. Kanamycin resistant colonies were further amplified and minipreps were performed. The presence of the desired mutations was confirmed by sequencing.

Inhibitors:
Jasplakinolide (J7473) and Taxol (Paclitaxel; P3456) were purchased from Thermo Fisher Scientific.

Generation of gene-edited HL-60 PAD4 Crispr cell line:
The generation of the PAD4 Crispr line was performed as described (4). The PAD4 guide RNA was designed using the sequence of the first exon of the human PAD4 gene and the Crispr.mit webtool from the Zhang Lab (http://crispr.mit.edu). The following guide RNA sequence was selected: Guide1: 3'->5' TC ACA CGG ATC AAT GTC CCC TGG. The selected guide RNA had a low score (<0.3) of possible exonic off-targets with more than 4 mismatches per sequence. The following oligos containing the guide RNA without the PAM sequence but with the 5'-CACC and the 5'-AAAC overhangs were used: Hm-Padi4-Exn1-1-Fw: 5'-CAC CGG GGA CAT TGA TCC GTG TGA-3'; Hm-Padi4-Exn1-1-Rv: 5'-AAA CTC ACA CGG ATC AAT GTC CCC-3'.
Oligos were phosphorylated with the T4 Polynucleotide Kinase (NEB, M0201S), annealed then ligated into the pSpCas9-2A-GFP vector using the T4 DNA ligase. The bacterial genomic DNA was removed using the Plasmid Safe exonuclease (Fischer Scientific, NC9046399) then the resulting sgRNA-pSpCas9-2A-GFP vector was transformed into One Shot® Stbl3™ Chemically Competent *E. coli* (Thermo Fischer, C737303). Ampicillin resistant colonies were further amplified, plasmid DNA was purified using the QIAprep Spin Miniprep Kit and the insertion and integrity of the guide RNA sequence was verified by sequencing using the LKO1 primer (5'-GAC TAT CAT ATG CTT ACC GT-3'). Validated sgRNA-pSpCas9-2A-GFP plasmid were amplified and

purified using the PureYield™ Plasmid Maxiprep System (Promega, A2393) to generate pSpCas9-2A-GFP_Padi4-sgRNA.

$5x10^6$ non-differentiated HL-60 cells at passage 5 (passage 0 being when cells were received from ATTC) were electroporated with 5 µg of the pSpCas9-2A-GFP_Padi4-sgRNA plasmid using the Amaxa nucleofector kit V and the program Y-001 in an Amaxa Nucleofector. 24 hours after transfection, GFP positive cells were sorted by flow cytometry into 348 well plates (1 cell/well). Clonal cells were expanded and differentiated with DMSO and PAD4 protein level verified by western blot. All the obtained 20 clones had some remaining PAD4 protein detectable by western blot. The clone with the lowest level of PAD4 protein was retained and used as the HL-60 PAD4 CR line.

Immunofluorescence:

Lamin and vimentin immunostaining of mouse PMN: Neutrophils freshly isolated from the blood of WT and PAD4 KO mice were resuspended in serum-free RPMI 1640 medium supplemented with 25 mM HEPES and 1% P/S and plated on cleaned coverslips (#1.5, 22 mm x 22 mm) on top of parafilm in 35 mm wells at 2.1 x 10^4 cells in 100 µL per coverslip. Cells were incubated at 37°C for 5 min to allow adherence before the addition of ionomycin (4 µM; Tocris, 1704) or vehicle (DMSO). After 4 hours, cells were fixed and permeabilized with anhydrous -20 °C methanol (Alfa Aesar 41838AK) for 10 minutes. Fixed cells were rinsed twice with 0.05% TWEEN 20 (Sigma, P1379) for 3 minutes each, followed by a third wash with phosphate buffered saline (PBS, Gibco, ThermoFisher, 20012027) for another 3 minutes, using 2 mL for each wash. Cells were then incubated with primary antibodies (rabbit anti-LB1/2 (1:1000; Abcam ab16048) or chicken anti-vimentin (1:250; Biolegend Poly29191)) for 1 hour at room temperature and rinsed again as described above. Next, samples were incubated with secondary antibodies (Alexa 488 goat anti-rabbit, 1:400, ThermoFisher, A-11008; or Alexa 568 goat anti-chicken, 1:400, ThermoFisher, A-11041) for an hour at room temperature and stained with either Hoescht 33258 (1:10000, Molecular Probes, H3569) or SiR-DNA (1 µM, Cytoskeleton, CY-SC007) and rinsed again. Stained cells were then mounted in Prolong Glass (ThermoFisher, P36982) and allowed to cure for 24 hours. Gentle vacuum suction was used between each step above to remove the solution from the prior step.

HL-60 and Human PMNs granule, lamin and vimentin immunostaining: 3x10^5 dHL-60 cells or Human PMNs were resuspended in 300 µL of culture media without FBS (RPMI 1640, 25 mM HEPES and 1% P/S) and plated on 22 x 22 mm #1.5 cleaned glass coverslips. Cells were left to adhere on coverslips for 10 minutes at 37°C and 5% CO_2 . For Human PMNs, 700 µL of culture media without FBS supplemented with 1 µL of DMSO or Ionomycin (4mM; for a final concentration of 4 µM) was added to coverslips then incubated for 5, 10, 60 or 240 minutes at 37°C and 5% CO_2. Indirect immunofluorescence was performed as already described (7). Briefly, cells were fixed for 20 minutes at 37°C with 4% paraformaldehyde (PFA; Electron Microscopy Science,15710) in cytoskeleton buffer (CB; 10 mM MES, 3 mM $MgCl_2$, 138 mM KCl, and 2 mM EGTA) then permeabilized with 0.5% of Triton X-100 in CB at 37°C for 5 minutes. Free aldehydes were quenched with 10 mM glycine in CB at room temperature (RT). Cells were washed once for 5 minutes followed by 2 x 10 minutes washes with Tris Buffered Saline (TBS; 20 mM Tris, pH 7.6, 137 mM $NaCl_2$) before being blocked for 1 hour at RT with blocking solution (2% BSA IgG free and protease free (Sigma-Aldrich, A3059); 0.1 % Tween 20 (Sigma-Aldrich, P1379) in TBS). Cells were stained for 2 hours at RT with primary antibodies (1:400) diluted in blocking solution then washed before being incubated with fluorophore-conjugated secondary antibodies (1:200), Alexa-Fluor-647 phalloidin (1:100; ThermoFisher, A22287) and Dapi (1ug/mL; Sigma, 268298) diluted in blocking solution, for 1 hour at RT. Cells were washed with blocking solution then with TBS (2 x 10 minutes, each). The coverslip was mounted on a glass slide in mounting media (Dako; Pathology Products, S3023) then sealed with nail polish. The following primary antibodies were used: rabbit anti-neutrophil elastase (Millipore, 481001-1ML), mouse anti-myeloperoxidase (Abcam, ab90810), mouse anti-lactoferrin (Abcam, ab10110), mouse anti-MMP9 (Abcam, ab58803), mouse anti-tetranectin (Abcam, ab51883), rabbit anti-lamin A/C (abcam, ab108595), rabbit anti-lamin B1 (abcam, ab16048), mouse anti-lamin B2 (abcam, ab8983), mouse anti-PAD4 (abcam, ab128086), rabbit anti-PAD4 (GeneTex, 113945), mouse anti-vimentin (Clone 091D3, Biolegend, 677801). The secondary antibodies Alexa Fluor 488 Donkey anti-rabbit (711-545-

152), Alexa Fluor 594 Donkey anti-rabbit (711-585-152), Alexa Fluor 488 Donkey anti-mouse (715-545-150) and Alexa Fluor 594 Donkey anti-mouse (715-585-150) were from Jackson Immunoresearch Laboratories.

PAD4 immunostaining of human PMNs: Fresh blood was collected from 3 human subjects into EDTA-coated vacutainers or capillaries, and 3-5 μL was immediately smeared onto microscope slides. The slides were allowed to air dry for 2-3 min, and then fixed in 100% methanol for 10 sec. After air dry for another 2-3 min, cells were fixed in 2% paraformaldehyde for 2 hours at room temperature. The slides were washed 3 times with PBS and permeabilized in 0.1% sodium citrate and 0.1% Triton X-100 in PBS for 10 min at 4°C. After a rinse in PBS, the slides were blocked in 3% BSA in PBS for 2 hr at room temperature in a humidified chamber. Primary antibodies diluted in 0.3% BSA with 0.05% Tween-20 in PBS (PBS-T-BSA) were added to the slides: (1) anti-PAD4 (1:500; Abcam, ab128086) plus anti-CD11b (1:250; Abcam, ab52478) or (2) anti-PAD4 (1:100; GeneTex, 113945) plus anti-CD66b (1:250; Biolegend, 305103), and incubated overnight at 4C. After two washes in PBS, appropriate Alexa Fluor-conjugated secondary antibodies were added to the slides at 1:1,500 diluted in PBS-T-BSA. The slides were then washed, counterstained for DNA using Hoechst 33342 (1:10,000) for 10 min at room temperature, and coverslips were mounted with FLUORO-GEL mounting medium (Electron Microscopy Sciences).

dHL-60 NETosis endpoint assay:

Differentiated HL-60 cells were pelleted, resuspended in serum-free RPMI 1640 medium buffered with 10 mM HEPES, and plated at 15,000 cells per well in 96-well plates. After 20 min of incubation to allow for adherence, cells were stimulated with ionomycin (4 μM) for 2.5 h, then fixed in 2% paraformaldehyde containing Hoechst 33342 (1:10,000; Invitrogen, H3570) at 4°C overnight. Fixed cells were imaged on a Zeiss Axiovert 200M wide-field fluorescence microscope. Percentage of NETs was quantified from 6 non-overlapping fields per well and the average was taken from triplicates in every experiment.

Western blot:

Western blots were performed as previously described (8). In brief, cells were lysed in Laemmli sample buffer, lysates were separated by SDS-PAGE and proteins were electro transferred overnight at 4°C to an Immobilon-P PVDF membrane. Membranes were blocked for 1 h at room temperature (RT) with 5% nonfat dry milk (wt/vol) in TBS-T buffer (TBS + 0.1% Tween-20 [vol/vol]) then incubated for 2 h at room temperature with indicated primary antibodies. Subsequently, membranes were washed 3 x 5 min in TBS-T, incubated with appropriate HRP-conjugated secondary antibodies (1:10,000) for 1h at room temperature then washed 3 x 5 min in TBS-T. An ECL detection system (Millipore) was used to visualize protein bands.

The following antibodies were used: mouse anti-PAD4 (1:1000; abcam, ab128086), rabbit anti-lamin A/C (1:1000; abcam, ab108595), rabbit anti-lamin B1 (1:1000; abcam, ab16048), mouse anti-lamin B2 (1:1000; abcam, ab8983), rabbit anti-Gapdh (1:2000; Clone 14C10, Cell Signaling, 2118S). The secondary antibodies (HRP-conjugated goat anti-mouse (115-035-003) or goat anti-rabbit (111-035-003)) were from Jackson ImmunoResearch Laboratories.

The relative level of PAD4 protein in CRSPR cell lines was quantified using ImageJ 1.52n (NIH) by first performing local background subtraction around the bands of interest, then calculating the ratio between the PAD4 intensity and the corresponding Gapdh intensity for both WT and PAD4 CR dHL-60 cells to obtain the PAD4 protein amount relative to the total protein content. For each repeat, the so normalized PAD4 intensity was further normalized to the WT dHL-60 level to obtain the percentage of PAD4 protein relative to WT.

Nitroblue tetrazolium (NBT) assay for reactive oxygen species production

The NBT assay was performed as described (9, 10). $2x10^6$ cells were washed two times in PBS at room temperature then resuspended in 1.5 mL of imaging media alone(-PMA; -NBT) or supplemented with 20 nM of phorbol-12-myristate-13-acetate (PMA) (+PMA; -NBT), 3 mg of NBT (ThermoFisher, N6495) (-PMA; +NBT), or 20 nM of PMA combined with 3 mg of NBT (+PMA; +NBT). Cells were then incubated for 25 minutes at 37°C and 5% CO_2 before being transferred on ice, washed three times in ice cold PBS then fixed with 100 μL of ice cold 2% PFA in PBS. Fixed cells were left overnight at 4°C before being analyzed by flow cytometry.

Flow cytometry was performed on an LSR II equipped with a BD FACSDiva™ software (BD Biosciences). Cells' side scatter area (SSC-A) as function of cells' forward scatter area (FSC-A) that measure cell granularity and size respectively plots were generated. Control cells (-PMA; -NBT) were first loaded to define the NBT<0 gate on the FSC/SSC plot and the new population with higher SSC-A detected by loading the (+PMA; +NBT) sample was used to define the NBT>0 gate. Samples were then run at medium flow rate and detection was stopped at 100.000 cells. The percentage of cells in the NBT<0 and NBT>0 was measured with the FACSDiva™ software.

Reverse Transcriptase Polymerase Chain Reaction (RT-PCR) for PADi4 mRNA detection. RNA from differentiated WT and PAD4 CR HL-60 cells was extracted using the RNeasy Mini Kit (Quiagen, 75104) as directed by the vendor. RT-PCR was performed using the AccessQuick™ RT-PCR System (Promega, A1701) as directed by the vendor with Gapdh as loading control. The following primers were used: PAD4 P1 Fw: 5'- ACT TCT TCA CAA ACC ATA CAC TGG-3'; PAD4 P1 Rev: 5'- CCT CGA GTT ACA TAG CCA AAA TCT-3'; PAD4 P2 Fw: 5'- GTG TTC CAA GAC AGC GTG GT -3'; PAD4 P2 Rev: 5'- GTT TGA TGG GAA ACT CCT TCA G-3'; GAPDH Fw: 5'-ACC CAG AAG ACT GTG GAT GG-3'; GAPDH Rev: 5'-CCC CTC TTC AAG GGG TCT AC-3'. The PCR product was separated by electrophoresis using a 1% agarose gel in Tris Acetate EDTA buffer stained with Midori green advance (1:20,000; Nippon Genetics, MG04). mRNA bands were visualized using the Ultraviolet mode of MyECL imager (ThermoFisher).

Microscopy:
Spinning disc confocal and DIC microscopy: Imaging was performed on a Nikon Eclipse Ti or Ti2 microscope equipped with Perfect Focus^{TM} equipped with a Yokogawa CSU-X1 or CSU-W1 spinning disc scanhead, a Hamamatsu Orca-flash 4.0 v2 or v3 camera and a Plan Apo 60x oil 1.4 NA DIC, an Apo Tirf 60x oil 1.49 NA DIC or an Apo Tirf 100x oil 1.49 NA DIC Nikon objective lens and the appropriate DIC prisms in place. Illumination was provided on the CSU-W1 by Nikon LUNV 6 line laser unit (20 mW 405nm; 20 mW 445nm; 70 mW 488nm; 40 mW 515nm; 70 mW 561nm and 40 mW 640nm; power measurement is at the fiber output) with 2 single mode optical fiber outputs (1 APC and 1 UPC on a fast actuator). Illumination on the CSU-X1 was provided by the Agilent MLC400B Monolithic Laser Combiner with four lasers (405nm: 20mW, 488nm: 50 or 80mW, 561nm: 50 or 80mW, 647nm: 125mW)). DIC illumination was provided by a 100W halogen bulb or LED using an 0.52 NA condenser lens. Microscopes were equipped with the Nikon motorized stage with xy linear encoders and a Mad City (Madison, WI) Nano-Z100 piezo insert with 200um travel. Laser confocal or DIC illumination were selected with electronic shutters and an automated filter turret containing a multibandpass dichromatic mirror together with an electronic emission filterwheel. Microscope functions were controlled by NIS-Elements software (Nikon).
For live cell imaging, cells were incubated with SiR-DNA (30 min at 0.5 or 1 µM; Cytoskeleton, CY-SC007), SiR-Actin (1 hour at 1 µM; Cytoskeleton, CY-SC001), SiR-Tubulin (1 hour at 1 µM; Cytoskeleton, CY-SC006) or ER-Tracker Red dye (30 min at 1 µM; ThermoFisher, E34250) at 37°C and 5% CO_2 before being washed then resuspended in 300 µL of imaging media. For assaying plasma membrane permeability cells were imaged in media containing 20 µM calcein (ThermoFisher, C481), 1 mg/mL of Alexa fluor 647 (ThermoFisher, D22914) or Alexa fluor 594 (ThermoFisher, D22913) 10 kDa dextran or Oregon Green 488 70 kDa dextran (ThermoFisher, D7172). For live annexin V recruitment, cells were resuspended in imaging media supplemented with annexin V- Alexa Fluor 488 (1 µM, Thermofisher, A13201).For *Candida albicans*-induced NETosis assays, Sytox Green (0.1 µM, Thermofisher, S7020) was added to imaging media to aid in visualization of cellular DNA release, which was difficult to see in images because of the highly refractile yeast. A non-coated, gamma-irradiated glass bottom 35 mm dish (WPI, FD35-100), 24-well plate (CellVis, P24-1.5H-N) or 4 Well chambered cover Glass (CellVis, C4-1.5H-N) was placed on a pre-warmed (37°C) microscope stage. Sample temperature and humidity were controlled with a Tokai Hit stage-top incubator (Tokai Hit) or a Pathology devices live cell stage-top incubator (Pathology Devices). Cells were plated on temperature-equilibrated glass bottom dishes and allowed to adhere for 5 minutes. Multiple (3 to 10) random fields containing multiple adherent cells were selected for imaging. Confocal and DIC images at the coverslip-cell interface and 3 µm above in the cell center were acquired for each position. The image acquisition was

paused 10 minutes after beginning, ionomycin (final concentration of 4 μM), lipopolysaccharide (LPS (Klebsiella pneumoniae) final concentration of 25 μg/mL; Sigma-Aldrich, H4268) or *Candida albicans* (MOI = 2) was added and imaging was resumed. Images sets of DIC, 488 nm (Calcein, Oregon Green dextran, EGFP and mEmerald excitation), 561 nm (AlexaFluor 594 dextran, mApple and ER-Tracker Red dye excitation) and 647 nm (Alexafluor 647 dextran, SiR-DNA, SiR-Actin and SiR-Tubulin excitation) captured in rapid succession were acquired every 1-2 minutes for 4 hours.
dHL-60 and Human PMNs that were immunostained for lamins and vimentin were imaged by spinning disc confocal microscopy with a Plan Apo 100x oil 1.4 NA Ph3, DM Nikon objective and a 0.85 NA Dry condenser. For each coverslip, multiples (3-6) random fields were selected and pairs of phase contrast and fluorescence confocal stacks were captured.
Laser scanning confocal microscopy: Mouse PMNs that were immunostained for vimentin and laminB1/2 were imaged using a Zeiss LSM 510 laser scanning confocal microscope (63X oil immersion, NA=1.4, WD = 0.17 mm, Zeiss 44 07 61 1101-274) by selecting random fields of view containing multiple cells. Representative z-stacks were captured and 405, 488, 543, and 633 nm laser lines were used as appropriate for the immunofluorescence and nucleic acid stains. Image fields of view were collected until more than 50 cells were counted per condition.
A Nikon A1R resonance-scanning confocal microscope equipped with a Nikon Apo 60x/1.4 oil λS DIC N2 objective lens and controlled by NIS-Elements software was used to image human PMNs immunostained for PAD4 and to performed fluorescence recovery after photobleaching (FRAP) of soluble in mEmerald expressed in HL-60 derived neutrophils. For FRAP experiments, the 488 nm laser was used to image mEmerald (acquired every 65 ms) using the resonance scanner, and photobleaching (1 sec) was performed with the galvanometer-based scanner.
Epifluorescence microscopy: dHL-60 cells fixed after the NETosis endpoint assay (see above) were imaged using an Axiovert 200M wide-field fluorescence microscope (Zeiss) coupled to an AxioCam MR3 monochromatic CCD camera (Zeiss) using a Zeiss Plan-Neofluar 20x/0.4 Corr Ph2 objective lens with the Zeiss AxioVision software.

Image Analysis
Quantification of the percentage and timing of cellular events during NETosis: Time-lapse spinning disc confocal and DIC and movies of cells stained with SiR-DNA were used to quantify the percentage and timing of the following events: Plasma membrane microvesicle shedding, defined as the release of vesicles from the cell periphery as seen in DIC movies; DNA de-condensation, defined as the decrease in SiR-DNA inhomogeneity as seen in confocal fluorescence movies; Nuclear rounding, defined as the establishment of a circular nuclear periphery as seen in DIC and confocal fluorescence color overlay movies; DNA release from the nucleus, defined as expansion of the DNA periphery outside of the nuclear boundaries into the cytosol as seen in DIC and confocal fluorescence color overlay movies; PM permeabilization, defined as a decrease in contrast at the cell periphery as seen in DIC movies; and NETosis, defined as expansion of DNA outside of the cell boundary as seen in DIC and confocal fluorescence color overlay movies. All adherent cells in imaging fields were included in the analysis of the percentage of cells undergoing an event while only cells that remained in the field for the entire duration of the movie were included in the quantification of the timing of events. Multiple imaging fields were analyzed for each condition until the number of cells per condition was equal or greater than 50. The timing of an event was defined as the first time point when the corresponding event was observed in the movies by eye.
For analysis of *C. albicans*-induced NETosis in human PMNs, phagocytosis was defined when a yeast cell was enclosed by a human PMN. PM permeabilization was assessed by using the decrease in DIC contrast as well as the initial increase in cellular Sytox Green signal.
For quantification of the timing of cytoskeletal disassembly, vesiculation of the endoplasmic reticulum (ER), and rupture of the lamin meshwork, inner (Lap2β) and outer (ER) nuclear membranes in dHL-60 cells, time-lapse spinning disc confocal DIC and fluorescence movies of cells transfected with the corresponding fluorescent-protein-tagged-cDNA were used. The timing of events was defined as follows; Actin disassembly: solubilization and decrease in the intensity of F-tractin-mApple; Microtubule disassembly: solubilization of Ensconsin-eGFP; Vimentin disassembly: solubilization of vimentin-mEmerald; ER vesiculation: appearance of discontinuities

and vesicles in the ER network (stained with ER-5-mEmerald); Lamin A, B1, inner and outer nuclear membrane rupture: appearance of a discontinuity in the lamin meshwork or nuclear membrane. Cytoskeletal disassembly and ER vesiculation were detected using the confocal plane at the coverslip-cell interface while discontinuities in the lamin meshwork, inner and outer nuclear membranes were detected using the confocal plane at the cell center (3 µm above the cell-coverslip interface).
For quantification of the percentage and timing of cellular events in WT and PAD4 CR dHL-60 cells transfected with mEmerald-C1, mEmerald-PAD4, mEmerald-PAD4-C645A or mEmerald-PAD4-K59A/K60A/K61A, only fluorescently labelled (and thus transfected) cells were taken into account.
Quantification of the Lamin meshwork rupture points: Time-lapse spinning disc confocal DIC and fluorescence movies of dHL-60 cells transiently transfected with LaminA-mEmerald and stained with SiR-DNA were performed. Images were acquired every 1-2 min and the number of rupture points was defined as the number of discontinuities in the lamin A staining at the nuclear periphery the first time that the discontinuities were detectable by eye. Because the lamin meshwork in these cells is intrinsically discontinuous, only new discontinuities from where DNA expanded were taken into account.
Analysis of vimentin and lamin in mouse PMNs: Cells were counted from the fields in two independent experiments following an identical protocol with a DMSO vehicle control along with 5, 10, 60, and 240 minute time points. Images were evaluated for the distribution of vimentin immunofluorescence and the continuity of lamin immunofluorescence. The evaluations were done by two separate experimentalists.
Analysis of human neutrophils for PAD4 localization: For quantification of mean nuclear/cytosolic PAD4 ratio, the mean intensity of PAD4 in the nucleus (delineated by Hoechst DNA staining and DIC for nucleus outline) was divided by mean intensity of PAD4 in the cytosol (with reference to Hoechst DNA staining and DIC for cell outline) after each was corrected by background subtraction.
Quantification of plasma membrane permeabilization: Quantification of the ratio between the intracellular and extracellular calcein or dextran was performed by measuring the mean fluorescence intensity of the corresponding dye in a fixed-size ROI inside and outside the cell and calculating their ratio over time. Time of calcein and dextran entry was defined as the first time point (as detectable by eye) when the intracellular fluorescence of the corresponding dye increased. The DIC channel was used to define cells' delimitations.
Quantification of Nuclear and cytosolic PAD4 and NLS: Measurement of the nuclear and cytoplasmic PAD4 and NLS intensity in dHL-60 cells was performed using time-lapse movies of cells stained with SiR-DNA and transiently co-transfected with PAD4-mEmerald and NLS-mCherry. The confocal slice at the cell center (3 µm above the cell-coverslip interface) was used. Fixed-area ROIs inside the nucleus (as defined by the SIR-DNA staining) or in the cytosol (as defined by the DIC channel) were used to measure the mean PAD4 and NLS intensity overtime. The resulting mean intensity values were plotted after background subtraction and normalization to the maximum value of the corresponding mean intensity vector.

Statistical analysis
All graphs were plotted using the GraphPad Prism software. Mann-Whitney and the Fisher's Exact test were used to determine the significance of the difference between two distributions of random (timing graphs) or Boolean variables (percentages graphs). Mann-Whitney tests were performed using GraphPad Prism and Fisher's Exact tests were done using R (version x64 3.5.1).

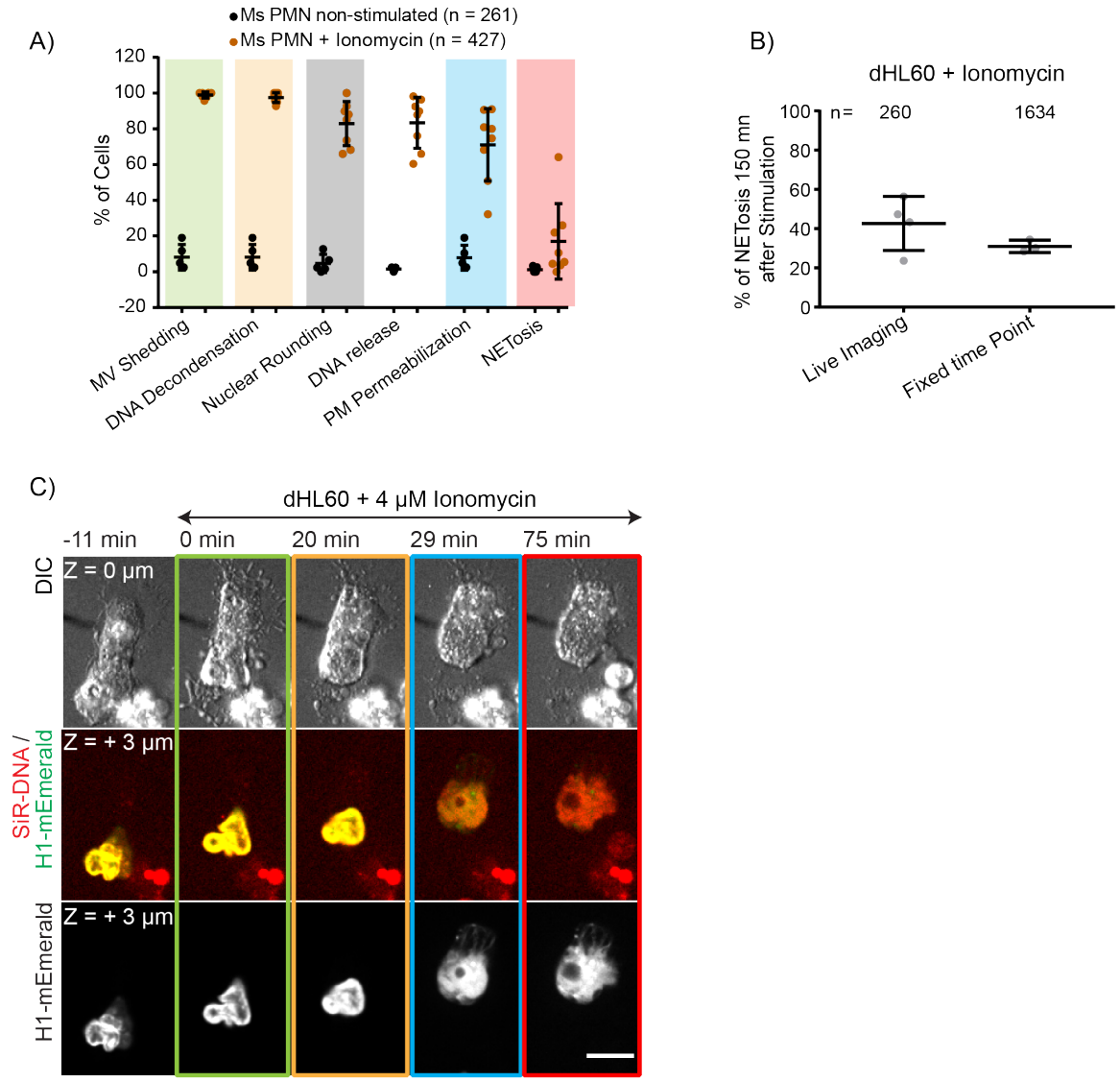

Fig. S1. Live-cell imaging is minimally disruptive to NETosis. Mouse PMNs and differentiated HL-60 neutrophil-like cells (dHL-60) were plated on coverslips, stimulated where indicated with 4 µM ionomycin, fixed and stained with DAPI after 150 min or imaged live by differential interference contrast (DIC) and spinning-disk confocal microscopy at the coverslip-cell interface (Z = 0 µm) and 3 µm above in the cell center (Z = + 3 µm) at 1-2 min intervals for 4 hours, with time in min relative to plasma membrane microvesicle shedding noted above images. Double-arrow-headed lines above images indicate cells that are in presence of ionomycin. A: Quantification of the percent of cells that exhibit microvesicle (MV) shedding, DNA de-condensation, nuclear rounding, release of nuclear DNA into the cytoplasm (DNA Release), loss of DIC contrast in the cell periphery suggesting plasma membrane permeabilization (PM Permeabilization), and extracellular DNA release (NETosis) after ionomycin stimulation or DMSO treatment determined from time-lapse DIC and confocal color-overlay movies. n = total number of cell observed, each point represents the percent of cells performing the event in one experiment, long bar = mean, short bars = S.D. Data for Ionomycin stimulated mouse PMNs was taken from figure 1B. B: Quantification of the percentage of cells that released extracellular DNA after 150 min in immunostaining experiments (fixed time point) or live cell imaging. n = total number of cells observed, each point represents the percent of cells in one experiment. long bar = mean, short bars = S.D. C: Time series of DIC (upper row) and fluorescence images of a live dHL-60 cell

stained with far-red SiR-DNA (middle row, red) and expressing histone H1 fused to mEmerald (middle and lower rows, green). Bar 10 μm. Boxes around images indicate different cellular events (green: MV Shedding; yellow: DNA De-condensation; blue: DNA release to the cytosol, red: extracellular DNA release).

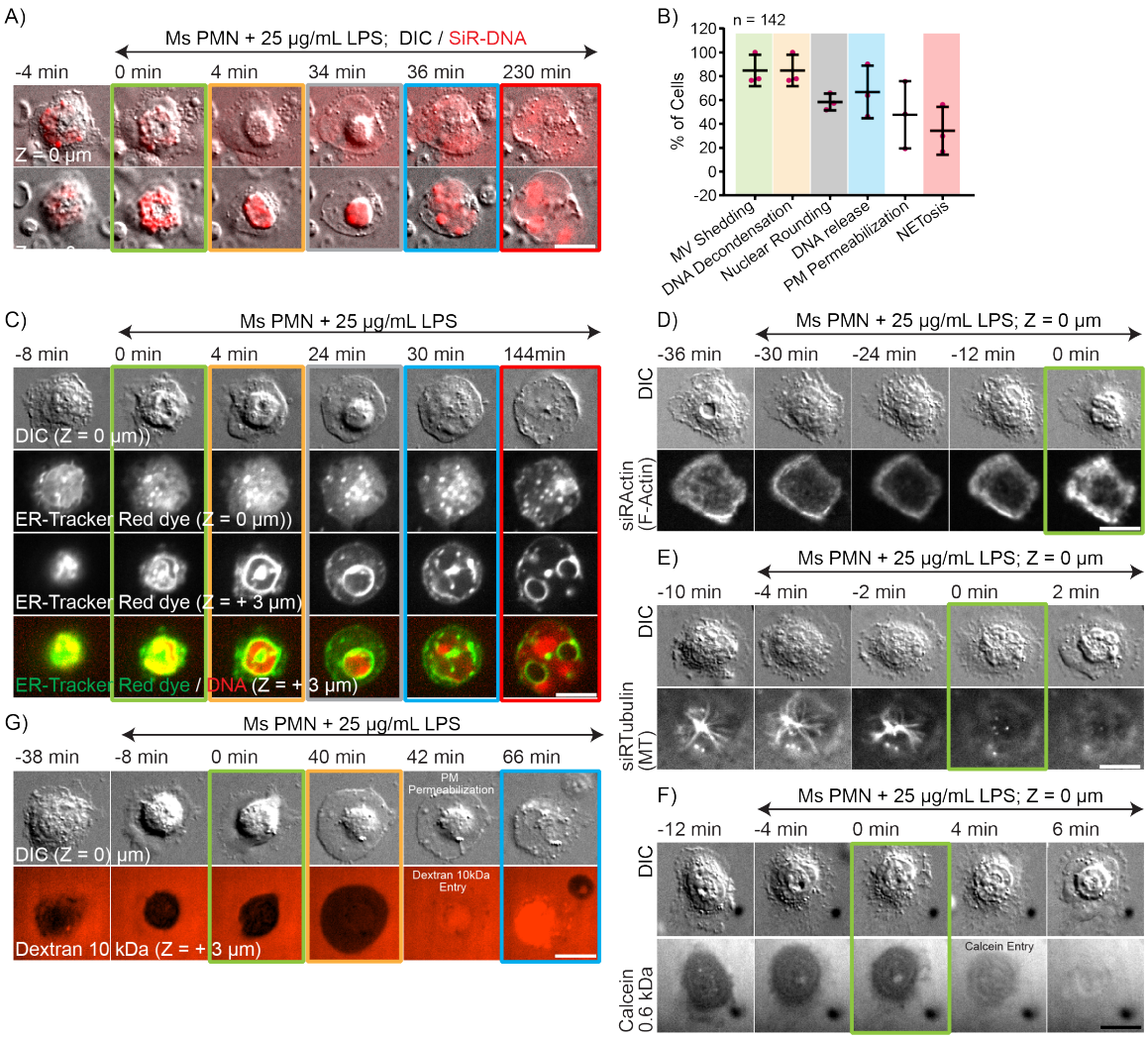

Fig. S2. Cellular events mediating NETosis in mouse neutrophils stimulated with LPS. Mouse blood polymorphonuclear neutrophils (Ms PMN) were plated on coverslips, stimulated with 25 µg/mL of lipopolysaccharides (LPS), and imaged live by differential interference contrast (DIC) and spinning-disk confocal microscopy at the coverslip-cell interface (Z = 0 µm) and 3 µm above in the cell center (Z = + 3 µm) at 2 min intervals for 4 hours, with time in min relative to plasma membrane microvesicle shedding noted above images. Double-arrow-headed lines above images indicate cells that are in presence of LPS, boxes around images indicate different cellular events (green: MV Shedding; yellow: DNA de-condensation; grey: nuclear rounding; blue: DNA release to the cytosol, red: extracellular DNA release). A: Time series of image overlays of DIC (greyscale) and fluorescence (red) of cell and DNA dynamics in far-red SiR-DNA stained cells. B: Quantification of the percent of cells that exhibit microvesicle (MV) shedding, DNA de-condensation, nuclear rounding, release of nuclear DNA into the cytoplasm (DNA Release), loss of DIC contrast in the cell periphery suggesting plasma membrane permeabilization (PM Permeabilization), and extracellular DNA release (NETosis) after LPS stimulation determined from time-lapse DIC and confocal color-overlay movies. n = total number of cell observed, each point represents the percent of cells performing the event in one experiment, long bar = mean, short bars = S.D. C-F: Time-series of DIC (top row) and confocal (lower rows) images of live cells. C: Cells were stained with ER-Tracker Red (middle rows and bottom row, green) to label the ER and the nuclear envelope (NE) and far red SiR-DNA (bottom rows, red) to label DNA. D,

E: Cells were stained with far red SiR-actin to fluorescently label actin filaments (D) or SiR-tubulin to fluorescently label microtubules (E). F, G: soluble fluorescent markers (calcein (622 Da, F, greyscale) or Alexa-fluor594 10 kDa dextran (G, red)) were added to the imaging media to monitor changes in plasma membrane permeability. A, C-F: bars= 10 μm.

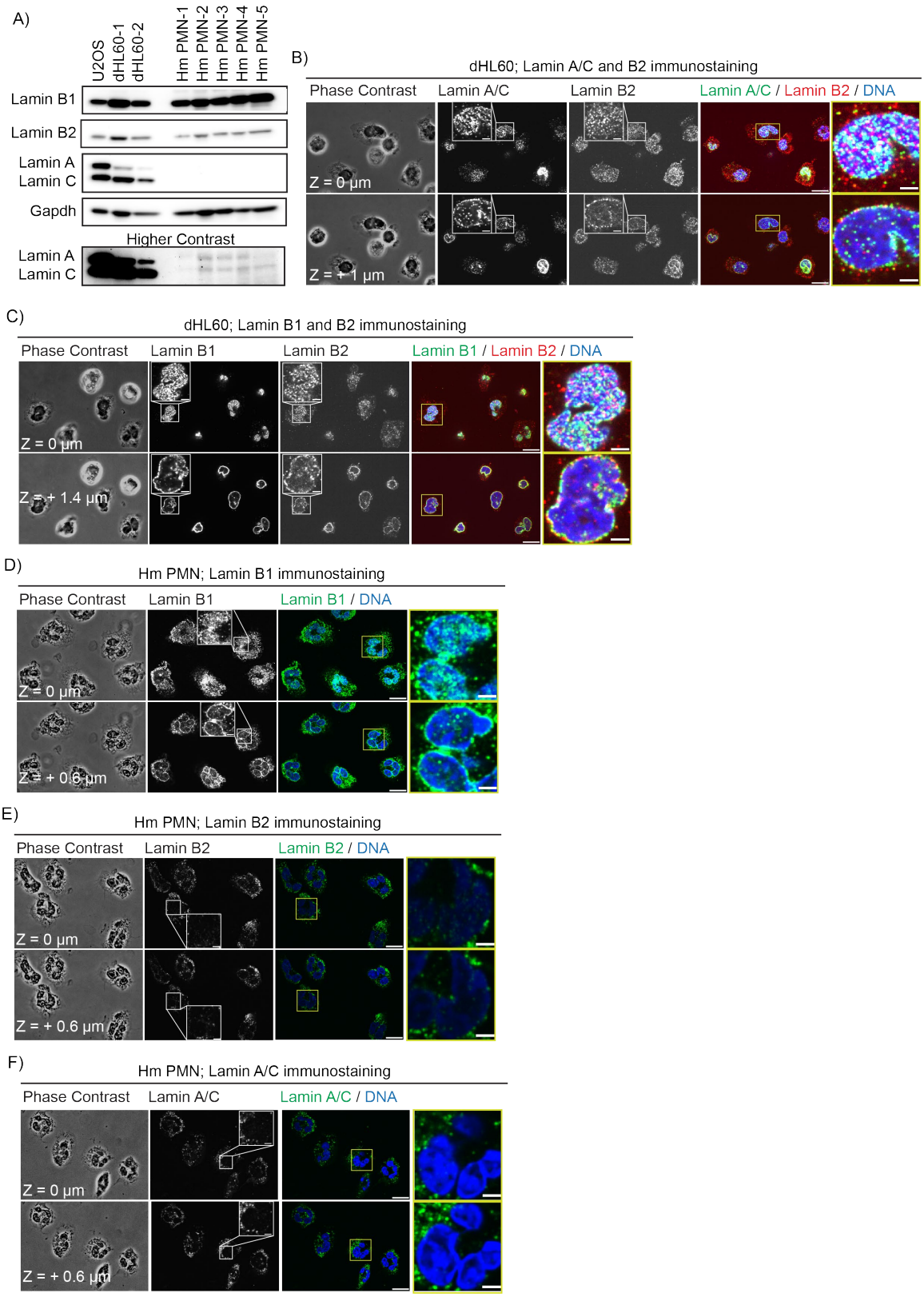

Fig. S3: Expression and localization of lamins in human blood neutrophils and dHL-60 cells. A: Western blot of lamin B1, B2 and A/C in lysates from human osteosarcoma cells

(U2OS), differentiated HL-60 neutrophil-like cells from 2 differentiation dates (dHL-60-1 and dHL-60-2) and human blood polymorphonuclear neutrophils from 5 different donors (Hm PMN-1- Hm PMN-5). GAPDH was used as loading control. Two different contrast settings of the image are shown (upper panel, lower contrast, lower panel, higher contrast) to highlight bands of different abundance. B-F: dHL-60 cells (B, C) or Hm PMN (D, E, F) were plated on coverslips for 5 minutes then fixed and immunostained for lamin A/C, B1, B2 and DAPI to label DNA as noted on images. Z-stacks of 0.2 μm steps were acquired on a spinning-disk confocal microscope, and the Z distance from the coverslip surface is noted on the image. B-C: cells were co-immunostained with lamin B2 and lamin A/C (B) or B1 (C). Insets show higher magnification of selected cells that are highlighted with a box. Color overlays are shown in the right-center and far right column, and the far right columns (outlined in yellow) show higher magnification of the boxed regions in the right-center columns. B-F: bars = 10 μm for lower magnification images and 2 μm for higher magnification images.

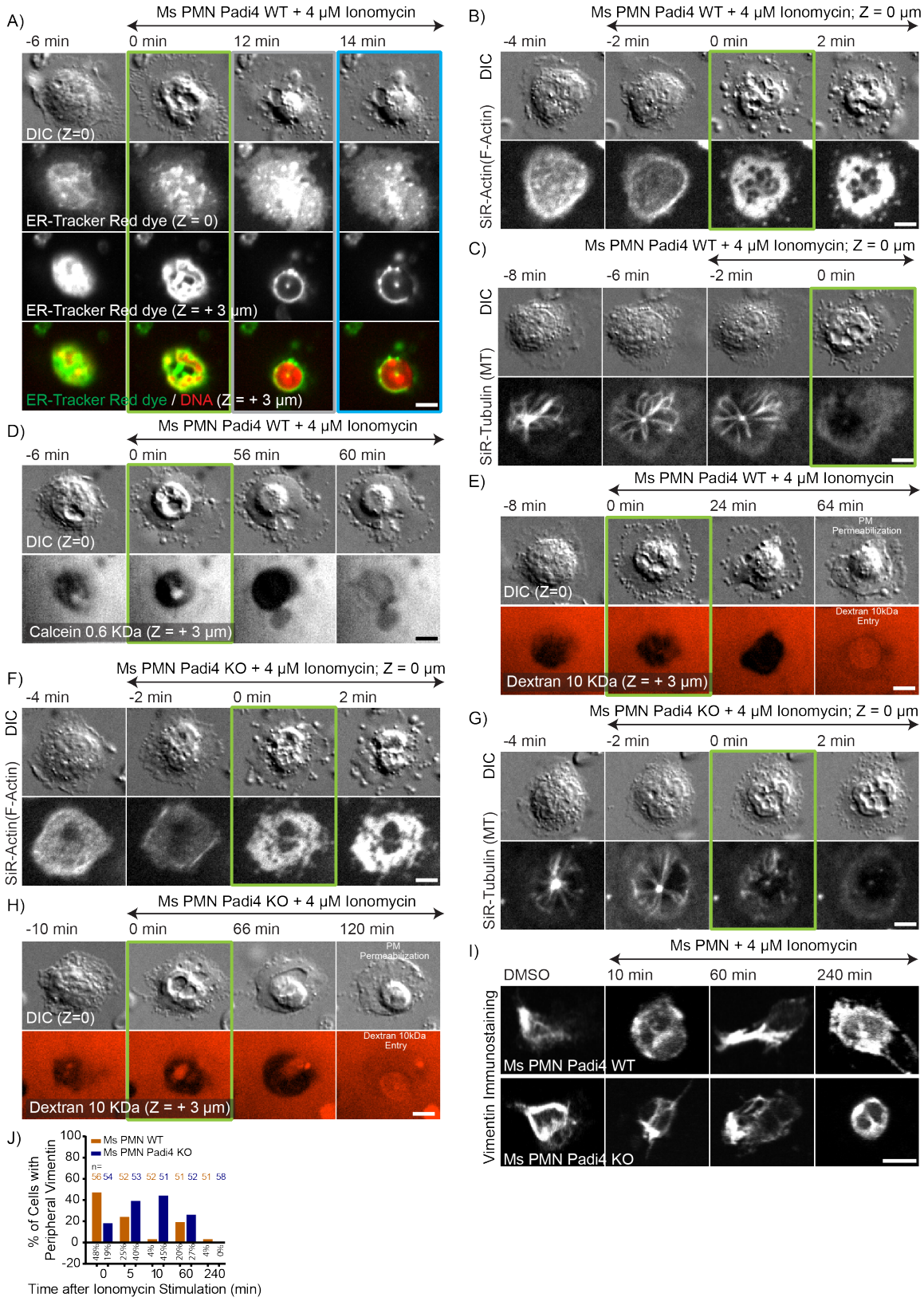

Fig. S4: Cytoskeletal disassembly/remodeling, ER vesiculation and increase in plasma membrane permeability occur independent of PAD4 in mouse neutrophils. Mouse blood

polymorphonuclear neutrophils (Ms PMN) from wild type (Padi4 WT) or PAD4 knockout (Padi4 KO) were plated on coverslips, stimulated with 4 μM ionomycin, and fixed (I, J) at different time points after stimulation (noted on images, I) or imaged live (A-H) by differential interference contrast (DIC) and spinning-disk confocal microscopy at the coverslip-cell interface (Z = 0 μm) and 3 μm above in the cell center (Z = + 3 μm) at 2 min intervals for 4 hours, with time in min relative to plasma membrane microvesicle shedding noted on images. Double-arrow-headed lines above images indicate cells that are in presence of ionomycin, boxes around images indicate different cellular events (green: MV Shedding; blue: DNA release to the cytosol) Loss of DIC contrast indicating plasma membrane permeabilization and cellular entry of 10 kDa fluorescent dextran are noted on images in E and H. A-H: Time-series of DIC (top row) and confocal (lower rows) images of live cells. A: Cells were stained with ER-Tracker Red (middle two rows and bottom row, green) to label the ER and nuclear envelope (NE) and far red SiR-DNA (bottom rows, red) to label DNA. B, C, F, G: Cells were stained with far red SiR-actin to fluorescently label actin filaments (B, F) or SiR-tubulin to fluorescently label microtubules (C, G). D, E, H: soluble fluorescent markers (calcein (622 Da, D, greyscale) or Alexa fluor 594 10 kDa dextran (E, H, red)) were added to the imaging media to monitor changes in plasma membrane permeability. I: Cells were fixed at the times shown after ionomycin stimulation and vimentin was immunolocalized. J: Quantification from immunostaining experiments of cells with peripheral vimentin at different time points after ionomycin stimulation. A-I: bars= 5 μm.

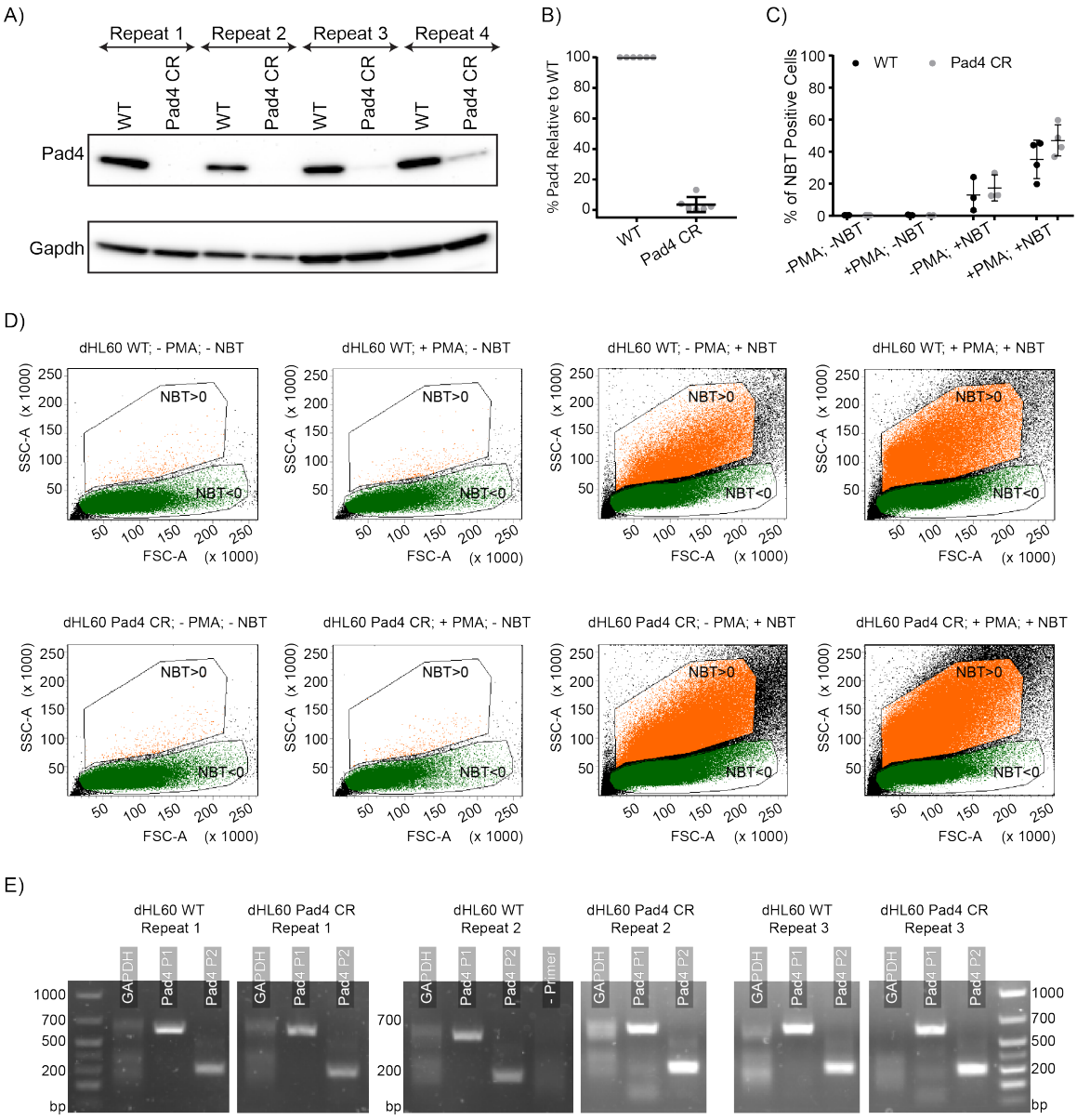

Fig. S5: Characterization of the PAD4 CR dHL-60 cell line. A: Western blot of PAD4 and GAPDH (as a loading control) for lysates of differentiated HL-60 neutrophil-like cells (dHL-60 WT) or dHL-60 with the PAD4 gene modified by CRSPR-Cas9 gene editing (PAD4 CR dHL-60) from four different differentiation dates (Repeat 1-4). B: Quantification from western blot experiments of the amount of PAD4 proteins expression relative to the WT levels in WT and PAD4 CR dHL-60 cells, each point represents a distinct experiment. C, D: WT and PAD4 CR dHL-60 cells were incubated in suspension for 25 min at 37C with DMSO or 20 nM Phorbol 12-myristate 13-acetate (PMA; +/-PMA) and +/- 2 mg/mL of Nitro blue Tetrazolium Chloride (NBT; +/-NBT) then fixed before being analyzed by flow cytometry. C: Quantification of the percentage of NBT positive cells (cells in the NBT>0 gate in panel D) as determined by the increase in cells' side-scatter signal. At least 100.000 cells were analyzed for each sample. D: Representative flow cytometry plots of cells' side scatter area (SSC-A) as function of cells' forward scatter area (FSC-A) that measure cell granularity and size respectively in WT (upper row) and PAD4 CR (bottom row) dHL-60 cells. Green dots: cells that did not reduce NBT (NBT<0 gate); orange dots: cells that reduced NBT (NBT>0 gate; higher SSC-A value); black dots represent cells that are excluded from our gating strategy. From left to right: control cells, cells treated with PMA; cells incubated with NBT only;

cells treated with PMA and incubated with NBT. E: RT-PCR of PAD4 and GAPDH mRNA in WT and PAD4 CR dHL-60 cells from 3 distinct differentiation dates (Repeat 1-3) using 2 different sets of primers with expected product sizes of 610 (PAD4 P1) and 298 (PAD4 P2) bp, respectively.

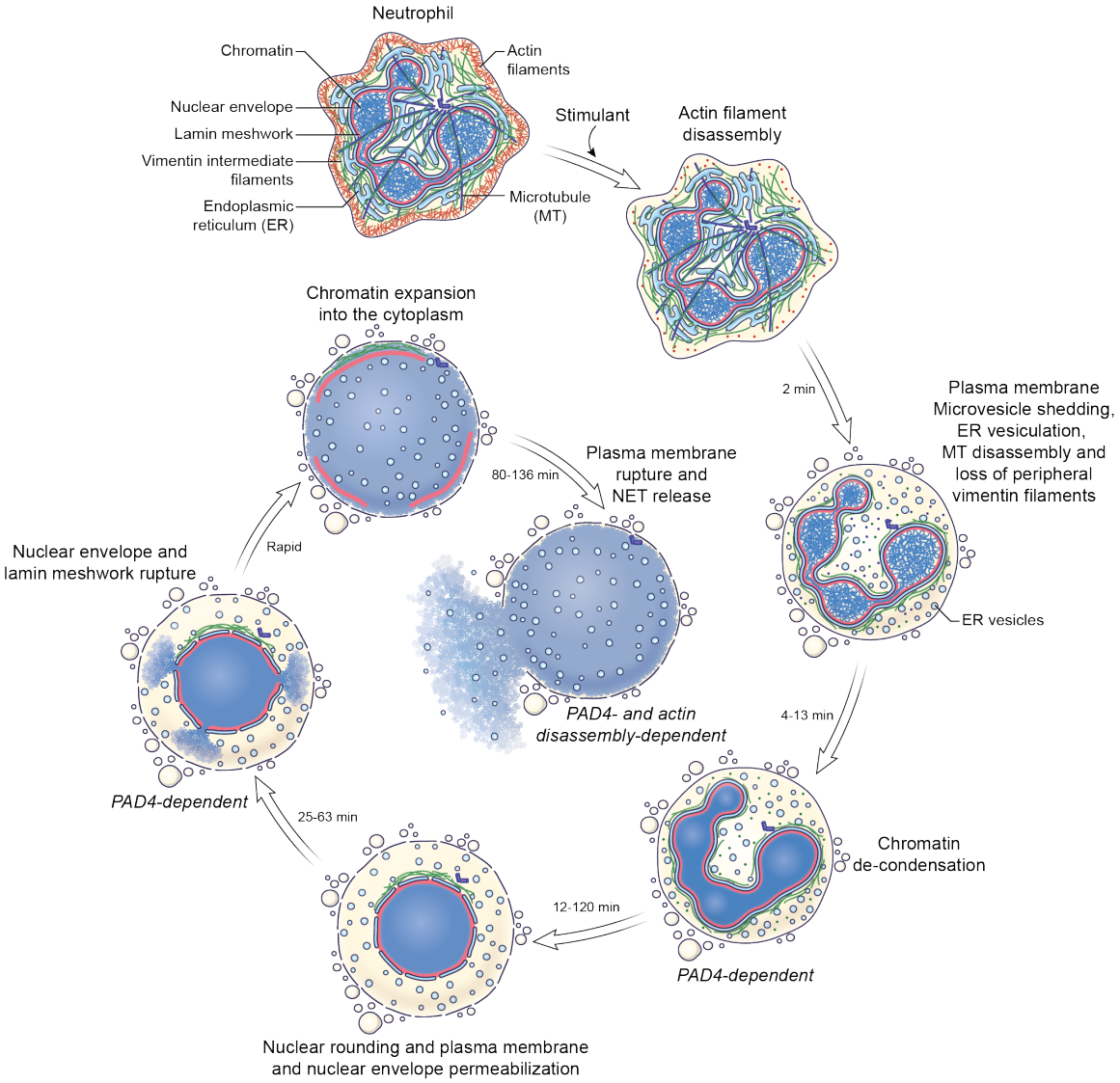

Fig. S6: Model of the cellular events mediating NETosis. Neutrophil (first panel) refers to mouse and human PMN and differentiated HL-60 neutrophil-like cells. Times are cumulative and relative to the initiation of actin cytoskeleton disassembly, ranges indicate the range of times for all three cell types.

Movie S1: Cell and DNA dynamics are similar in mouse and human PMN and dHL-60 cells during NETosis.

Mouse (Ms) or human (Hm) PMN or differentiated neutrophil-like (dHL-60) cells were stained with far-red SiR-DNA (red) and time-lapse DIC and spinning-disk confocal images were taken at one (dHL-60) or two (Ms and Hm PMNs) min intervals at the coverslip surface (Z = 0 μm) and at three microns above (Z= +3 μm). Cells were stimulated with dTomato-expressing *Candida albicans* (MOI=2, cyan) or 4 μM ionomycin or 25 μg/mL of lipopolysaccharides (LPS) at the timepoint when the labels appear. Sytox green (0.1 μM, green) was added to imaging media to better visualize extracellular DNA release in *C. albicans*-stimulated Hm PMN. White arrowheads highlight the *C. albicans* of interest. Elapsed time shown in min relative to plasma membrane vesiculation. Scale bar = 5 μm.

Movie S2: Cell, plasma membrane, and chromatin dynamics during NETosis in dHL-60 cells.

Differentiated neutrophil-like (dHL-60) cells were stained with far-red SiR-DNA (red, right panel) and co-transfected with the farnesylation signal sequence CAAX fused to mApple (CAAX-mApple, center panel) as a plasma membrane marker and histone H1 fused to mEmerald (H1-mEm, green, right panel) and time-lapse DIC and spinning-disk confocal images were taken every min. Cells were stimulated with 4 μM ionomycin at the timepoint when the label appears. Elapsed time shown in min relative to plasma membrane vesiculation. Scale bar = 10 μm.

Movie S3: Rapid drop in cytoplasmic refractive index suggests plasma membrane permeabilization during NETosis dHL-60 cells.

Differentiated neutrophil-like (dHL-60) cells were stained with far-red SiR-DNA (red) and time-lapse DIC and spinning-disk confocal images were taken every min at three microns above the coverslip surface (Z= +3 μm). Cells were stimulated with 4 μM ionomycin at the timepoint when the label appears. Right panel shows a zoom of the image on the left. Timepoint of drop in refractive index noted (PM Permeabilization). Elapsed time shown in min relative to plasma membrane vesiculation. Scale bar = 5 μm (left) or 2 μm (right).

Movie S4: Microvesicles are shed by cells undergoing NETosis.

Differentiated neutrophil-like (dHL-60) cells were transfected with mEmerald (middle panel; green, right panel) and stimulated with 4 μM ionomycin at the timepoint when the label appears. Time-lapse DIC and resonant laser scanning confocal images were taken every 0.07 sec. Bleaching was done with a galvanometer-based scanner for 0.97 sec. Elapsed time shown in sec relative to the beginning of photobleaching. Cyan arrows indicate photobleached regions (top: microvesicle; bottom: cell body). Scale bar = 2 μm.

Movie S5: Microvesicles contain phosphatidylserine

Differentiated neutrophil-like (dHL-60) cells were resuspended in imaging media supplemented with 1 μM annexin V-AlexaFluor488 (grey in middle panel, red hot color scale in left panel) and stimulated with 4 μM ionomycin at the timepoint when the label appears. Time-lapse DIC and spinning-disk confocal images were taken every min. Elapsed time shown in min relative to plasma membrane vesiculation. Cyan rectangles indicate the zoomed region shown in the right panel. Scale bar = 5 μm.

Movie S6: Lamin meshwork rupture during NETosis in dHL-60 cells.

Differentiated neutrophil-like (dHL-60) cells were stained with far-red SiR-DNA (red, right panels) and transfected with either mEmerald (green) fused to either lamin A (upper row) or lamin B

(lower row). Time-lapse DIC and spinning-disk confocal images were taken at one min (for lamin A) or two min (for lamin B1) intervals at three microns above the coverslip surface (Z= +3 μm). Cells were stimulated with 4 μM ionomycin at the timepoint when the label appears. Cyan arrowheads highlight rupture initiation points. Elapsed time shown in min relative to plasma membrane vesiculation. Scale bars = 5 μm.

Movie S7: Endoplasmic reticulum (ER) vesiculation during NETosis in mouse and human PMN and dHL-60 cells.

Mouse (Ms) or human (Hm) PMN were stained with ER-Tracker Red vital dye and differentiated neutrophil-like (dHL-60) cells were transfected with the KDEL sequence combined with the ER-retention signal sequence from calreticulin fused to mEmerald (ER-5-mEmerald) and time-lapse DIC and spinning-disk confocal images were taken at 2 min (for human and mouse PMN) or 1 min (for dHL-60) intervals at the coverslip surface (Z = 0 μm). Cells were stimulated with 4 μM ionomycin or 25 μg/mL lipopolysaccharides (LPS) at the timepoint when the labels appear. Elapsed time shown in min relative to plasma membrane vesiculation. Scale bars = 10 μm.

Movie S8: Nuclear envelope rupture during NETosis in human PMN and dHL-60 cells.

Human (Hm) PMN were stained with far-red SiR-DNA (Red, right column) and ER-Tracker Red vital dye (green, bottom left) and differentiated neutrophil-like (dHL-60) cells were stained with far-red SiR-DNA (Red, right column) and transfected with either the inner nuclear envelope protein Lap2β fused to mEmerald (green, upper right) or the KDEL sequence combined with the ER-retention signal sequence from calreticulin fused to mEmerald (ER-mEmerald, green, middle right). Time-lapse DIC and spinning-disk confocal images were taken at one min (for Lap2β-mEmerald and ER-mEmerald) or two min (for ER-tracker dye) at 3 μm above the coverslip surface (Z = +3 μm). Cells were stimulated with 4 μM ionomycin at the timepoint when the labels appear. Arrowheads highlight rupture initiation points. Elapsed time shown in min relative to plasma membrane vesiculation. Scale bars = 5 μm (top and middle row) or 10 μm (bottom row).

Movie S9: Nuclear envelope and lamin meshwork rupture during NETosis in dHL-60 cells.

Differentiated neutrophil-like (dHL-60) cells stained with far-red SiR-DNA (blue) and co-transfected with the inner nuclear envelope protein Lap2β fused to mEmerald (green) and lamin B1 fused to mApple (red) and time-lapse DIC and spinning-disk confocal images were taken every min at 3 μm above the coverslip surface (Z = +3 μm). Cells were stimulated with 4 μM ionomycin at the timepoint when the labels appear. Arrowheads highlight rupture initiation points. Elapsed time shown in min relative to plasma membrane vesiculation. Scale bar = 5 μm.

Movie S10: Cytoskeletal remodeling and disassembly during NETosis in human PMN.

Human (Hm) PMN were stained with far-red SiR-Actin or SiR-Tubulin to label actin and microtubules, respectively, and time-lapse DIC and spinning-disk confocal images were taken every 2 min at the coverslip surface (Z = 0 μm). Cells were stimulated with 4 μM ionomycin at the timepoint when the labels appear. Elapsed time shown in min relative to plasma membrane vesiculation. Scale bar = 10 μm.

Movie S11: Cytoskeletal remodeling and disassembly during NETosis in mouse PMN.

Mouse (Ms) PMN were stained with far-red SiR-Actin or SiR-Tubulin to label actin and microtubules, respectively, and time-lapse DIC and spinning-disk confocal images were taken every 2 min at the coverslip surface (Z = 0 μm). Cells were stimulated with 4 μM ionomycin or 25

μg/ml lipopolysaccharides (LPS) at the timepoint when the labels appear. Elapsed time shown in min relative to plasma membrane vesiculation. Scale bar = 10 μm.

Movie S12: Cytoskeletal remodeling and disassembly during NETosis in dHL-60 cells.

Differentiated neutrophil-like (dHL-60) cells were transfected with F-tractin-mApple to label actin filaments, vimentin-mEmerald, or the microtubule-binding domain of ensconsin fused to eGFP (Ensconsin-eGFP) to lable microtubules. Time-lapse DIC and spinning-disk confocal images were taken at 15 sec (for F-tractin) or one min (for vimentin and ensconsin) intervals at the coverslip surface (Z = 0 μm). Cells were stimulated with 4 μM ionomycin at the timepoint when the labels appear. Elapsed time shown in min relative to plasma membrane vesiculation. Scale bar = 5 μm.

Movie S13: Jasplakinilode blocks actin disassembly and inhibits NET release in dHL-60 cells.

Differentiated neutrophil-like (dHL-60) cells were transfected with actin-mEmerald (G-actin-mEmerald, green) and stained with far-red SiR-DNA (red) and time-lapse DIC and spinning-disk confocal images were taken every two min at the coverslip surface (Z = 0 μm) and three microns above the coverslip surface (Z = +3 μm) in the absence (top row) or presence (bottom two rows) of 1 μM jasplakinolide. Two examples of jasplakinolide-treated cells are shown: one in which the cortical actin blocks NET release (middle row) and one in which the NET is released at a gap in the cortical actin (bottom row). Cells were stimulated with 4 μM ionomycin at the timepoint when the labels appear. Elapsed time shown in min relative to plasma membrane vesiculation. Scale bar = 5 μm.

Movie S14: Taxol blocks microtubule disassembly but does not affect NET release in dHL-60 cells.

Differentiated neutrophil-like (dHL-60) cells were transfected with tubulin-mEmerald (green) and stained with far-red SiR-DNA (red) and time-lapse DIC and spinning-disk confocal images were taken every two min at the coverslip surface (Z = 0 μm) and three microns above the coverslip surface (Z = +3 μm) in the absence (top row) or presence (bottom row) of 10 μM taxol. Cells were stimulated with 4 μM ionomycin at the timepoint when the labels appear. Elapsed time shown in min relative to plasma membrane vesiculation. Scale bar = 5 μm.

Movie S15: Plasma membrane ruptures at NET release in dHL-60 cells.

Differentiated neutrophil-like (dHL-60) cells were transfected with the farnesylation signal sequence CAAX fused to mApple (CAAX-mApple) as a plasma membrane marker and stained with far-red SiR-DNA (red) and time-lapse DIC and spinning-disk confocal images were taken every two min at three microns above the coverslip surface (Z = +3 μm). Cells were stimulated with 4 μM ionomycin at the timepoint when the labels appear. Elapsed time shown in min relative to plasma membrane vesiculation. Scale bar = 5 μm.

Movie S16: Plasma membrane permeabilizes prior to NET release in dHL-60 cells.

Differentiated neutrophil-like (dHL-60) cells were subjected to time-lapse DIC and spinning-disk confocal images taken every two min at the coverslip surface (Z = 0 μm) in media containing calcein (622 Da, top row) or Alexa fluor 647 10 kDa dextran (bottom row). Cells were stimulated with 4 μM ionomycin at the timepoint when the labels appear. Elapsed time shown in min relative to plasma membrane vesiculation. Scale bar = 5 μm.

Movie S17: Stepwise increase in plasma membrane permeability prior to NET release in human PMN and dHL-60 cells.

Human (Hm) PMN (top row) and differentiated neutrophil-like (dHL-60) cells (bottom row) were subjected to time-lapse DIC and spinning-disk confocal images taken every one or two min at the coverslip surface (Z = 0 µm) in media containing calcein (622 Da) and Alexa fluor 594 10 kDa dextran (red, top row) or Alexa fluor 647 10 kDa dextran (red) and Oregon Green 488 70 kDa (green, bottom row). Cells were stimulated with 4 µM ionomycin at the timepoint when the labels appear. Elapsed time shown in min relative to plasma membrane vesiculation. Scale bar = 10 µm.

Movie S18: Comparison of cell and DNA dynamics in wild type and PAD4 KO mouse PMN during NETosis.

Wild-type (WT) and PAD4 knockout (Padi4 KO) mouse (Ms) PMN were stained with far-red SiR-DNA (red) and time-lapse DIC and spinning-disk confocal images were taken at two min intervals at the coverslip surface (Z = 0 µm) and at three microns above (Z= +3 µm). Cells were stimulated with 4 µM ionomycin at the timepoint when the labels appear. Elapsed time shown in min relative to plasma membrane vesiculation. Scale bar = 5 µm.

Movie S19: Comparison of endoplasmic reticulum and nuclear envelope dynamics in wild type and PAD4 KO mouse PMN during NETosis.

Wild-type (WT) and PAD4 knockout (Padi4 KO) mouse (Ms) PMN were stained with far-red SiR-DNA (red) and ER-Tracker Red vital dye (green) and time-lapse DIC and spinning-disk confocal images were taken at two min intervals at the coverslip surface (Z = 0 µm) and at three microns above (Z= +3 µm). Cells were stimulated with 4 µM ionomycin at the timepoint when the labels appear. Elapsed time shown in min relative to plasma membrane vesiculation. Scale bar = 5 µm.

Movie S20: PAD4 dynamics in dHL-60 cells during NETosis.

Differentiated neutrophil-like (dHL-60) cells were transfected with PAD4-mEmerald (green) and mCherry fused to the nuclear localization signal sequence which served as a soluble nucleoplasmic marker (NLS-mCherry) and stained with far-red SiR-DNA (blue). Time-lapse DIC and spinning-disk confocal images were taken every two min at the coverslip surface (Z = 0 µm) and at three microns above the coverslip surface (Z = +3 µm). Cells were stimulated with 4 µM ionomycin at the timepoint when the labels appear. Elapsed time shown in min relative to plasma membrane vesiculation. Scale bar = 10 µm.

Movie S21: Comparison of cell and DNA dynamics in wild type and PAD4 CR dHL-60 cells during NETosis.

Differentiated neutrophil-like (dHL-60) cells (WT) and dHL-60 cells with PAD4 modified by gene editing (Pad4 CR) were stained with far-red SiR-DNA (red) and time-lapse DIC and spinning-disk confocal images were taken at one min intervals at the coverslip surface (Z = 0 µm) and at three microns above (Z= +3 µm). Cells were stimulated with 4 µM ionomycin at the timepoint when the labels appear. Elapsed time shown in min relative to plasma membrane vesiculation. Scale bar = 10 µm.

Movie S22: The enzymatic and nuclear localization activities of PAD4 are required for NETosis in dHL-60 cells.

Differentiated neutrophil-like cells with PAD4 modified by gene editing (dHL-60 Pad4 CR) were transfected with mEmerald (mEmerald-C1, green, first column) or mEmerald-tagged PAD4

(mEmerald Pad4, green, second column) or mEmerald-tagged PAD4 variants bearing point mutations coding amino acid substitutions that specifically inactivate its enzymatic activity (mEmerald-PAD4-C645A, green, third column) or nuclear localization signal (mEmerald-Pad4-K59A/K60A/K61A) were stained with far-red SiR-DNA (red) and time-lapse DIC and spinning-disk confocal images were taken at two min intervals at the coverslip surface (Z = 0 μm) and at three microns above (Z= +3 μm). Cells were stimulated with 4 μM ionomycin at the timepoint when the labels appear. Elapsed time shown in min relative to plasma membrane vesiculation. Scale bar = 10 μm.

SI References

1. A. Millius, O. D. Weiner, Manipulation of neutrophil-like HL-60 cells for the study of directed cell migration. *Methods Mol. Biol. Clifton NJ* **591**, 147–158 (2010).
2. S. L. Wong, *et al.*, Diabetes primes neutrophils to undergo NETosis, which impairs wound healing. *Nat. Med.* **21**, 815–819 (2015).
3. V. Brinkmann, B. Laube, U. Abu Abed, C. Goosmann, A. Zychlinsky, Neutrophil extracellular traps: how to generate and visualize them. *J. Vis. Exp. JoVE* (2010) https:/doi.org/10.3791/1724.
4. F. A. Ran, *et al.*, Genome engineering using the CRISPR-Cas9 system. *Nat. Protoc.* **8**, 2281–2308 (2013).
5. K. Arita, *et al.*, Structural basis for Ca^{2+}-induced activation of human PAD4. *Nat. Struct. Mol. Biol.* **11**, 777–783 (2004).
6. K. Nakashima, T. Hagiwara, M. Yamada, Nuclear localization of peptidylarginine deiminase V and histone deimination in granulocytes. *J. Biol. Chem.* **277**, 49562–49568 (2002).
7. A. M. Pasapera, I. C. Schneider, E. Rericha, D. D. Schlaepfer, C. M. Waterman, Myosin II activity regulates vinculin recruitment to focal adhesions through FAK-mediated paxillin phosphorylation. *J. Cell Biol.* **188**, 877–890 (2010).
8. A. M. Pasapera, *et al.*, Rac1-dependent phosphorylation and focal adhesion recruitment of myosin IIA regulates migration and mechanosensing. *Curr. Biol. CB* **25**, 175–186 (2015).
9. S. J. Collins, F. W. Ruscetti, R. E. Gallagher, R. C. Gallo, Normal functional characteristics of cultured human promyelocytic leukemia cells (HL-60) after induction of differentiation by dimethylsulfoxide. *J. Exp. Med.* **149**, 969–974 (1979).
10. O. C. Blair, R. Carbone, A. C. Sartorelli, Differentiation of HL-60 promyelocytic leukemia cells monitored by flow cytometric measurement of nitro blue tetrazolium (NBT) reduction. *Cytometry* **6**, 54–61 (1985).